

Supporting Information

Highly Stretchable, Self-adhesive, Ambient-stable, and Wide-temperature Adaptable Hydrophobic Ionogels for Wearable Strain Sensor

Jiahang Liu,^{†,#} Xuemeng Yang,^{†,#} Min Xu,[†] Hongnan Zhu,[†] Yan Cheng,[†] Shuaijie, Li,[†] Tianci Li,[†] Yunhong Jiao,^{†,*} and Hongzan Song^{†,*}

[†]College of Chemistry & Environmental Science, Hebei University, Baoding, Hebei Province, 071002, P. R. China

*Corresponding Authors

E-mails: jiaoyunhonghb@163.com (Y. J.); songhongzan@iccas.ac.cn (H. S.)

Table S1 Composition of the ionogels

Samples	Amount of DAAM/ <i>wt%</i>	Amount of BMIMTFSI/ <i>wt%</i>	Amount of HP-A in DAAM/ <i>wt%</i>
10%-Ionogel-1	10	90	0.2
10%-Ionogel-2	10	90	0.5
10%-Ionogel-3	10	90	1
10%-Ionogel-4	10	90	2
10%-Ionogel-5	10	90	5
15%-Ionogel-1	15	85	0.2
20%-Ionogel-1	20	80	0.2
20%-Ionogel-2	20	80	0.5
20%-Ionogel-3	20	80	1
20%-Ionogel-4	20	80	2
20%-Ionogel-5	20	80	5

Table S2 Mechanical properties of the ionogels

Samples	Elongation at break (%)	Tensile strength (kPa)	Young's modulus (kPa)	Toughness (kJ/m ³)
10%-Ionogel-1	1090	98.9	15	420.5
15%-Ionogel-1	1120	126.9	25	761.2
20%-Ionogel-1	1170	142.1	38	872.6
20%-Ionogel-2	830	158.5	188	745.7
20%-Ionogel-3	330	119.1	255	206.0
20%-Ionogel-5	85	59.1	365	26.9



WCA=92.7°

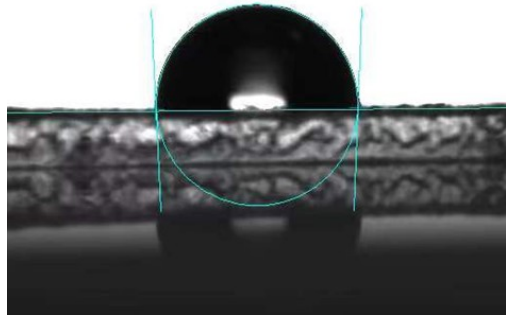


Fig. S1 Photographs showing the WCA of the surface of hydrophobic ionogel.

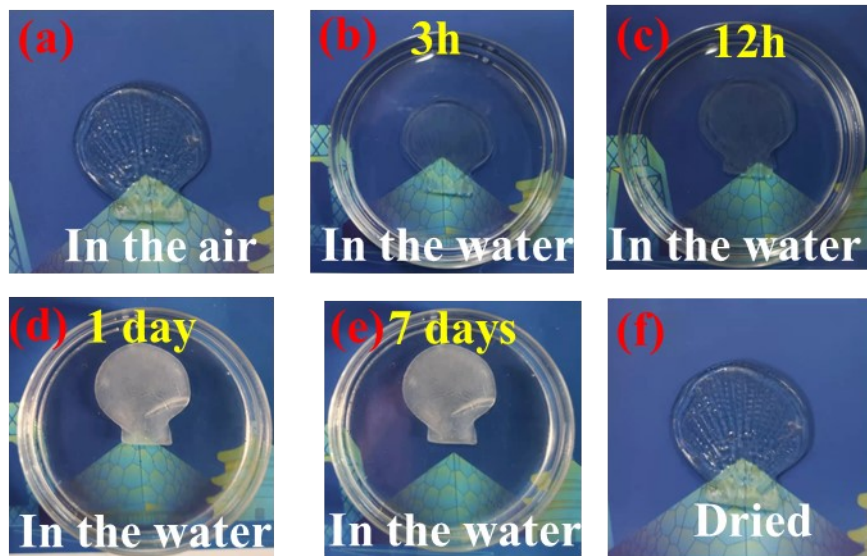


Fig. S2 Digital pictures of the ionogels in air (a), under water with different time (b-e), and the dried sample (f).

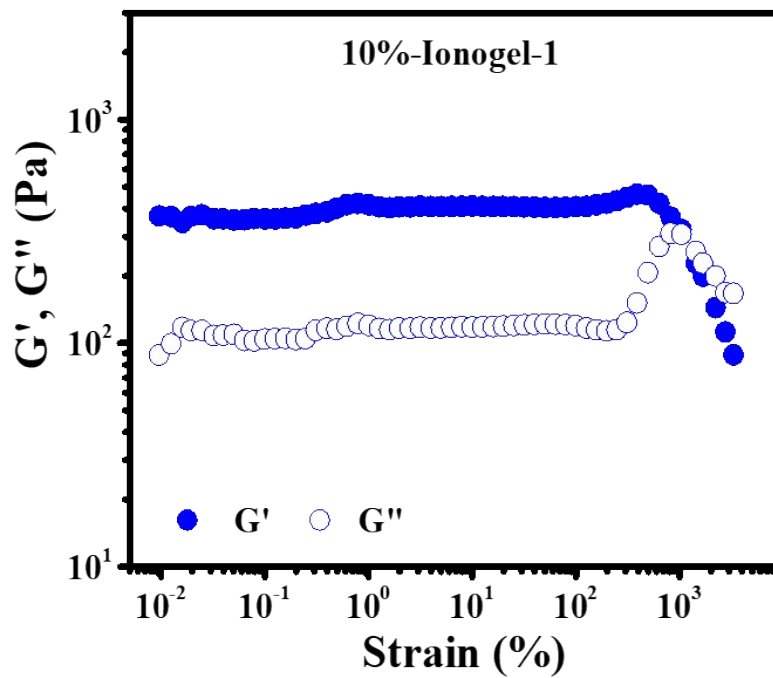


Fig. S3 Strain sweep curve of the sample 10%-Ionogel-1.

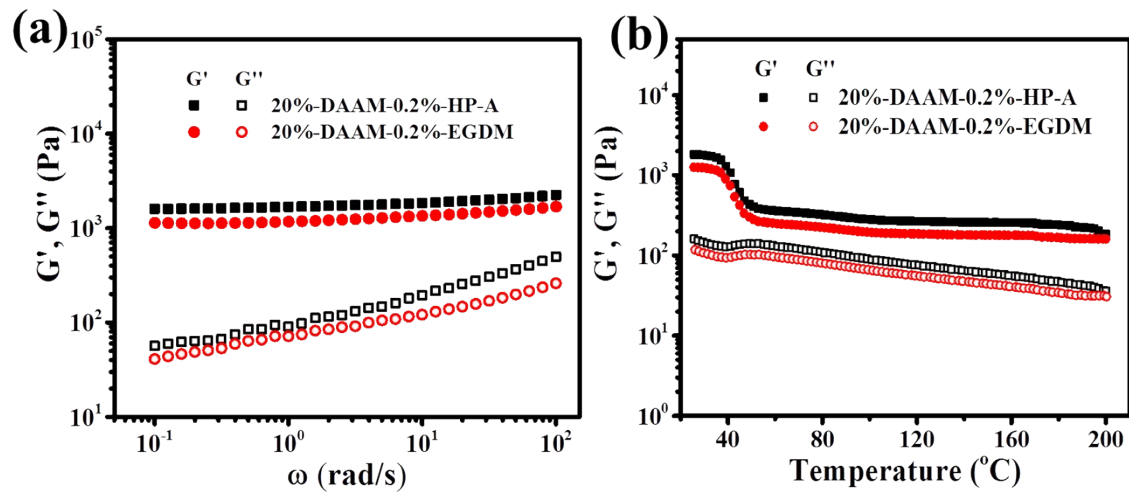


Fig. S4 (a) Changes of G' and G'' with frequency for the 20%-Ionogel with HP-A and EGDM. (b) Changes of G' and G'' with temperature for the 20%-Ionogel with HP-A and EGDM.

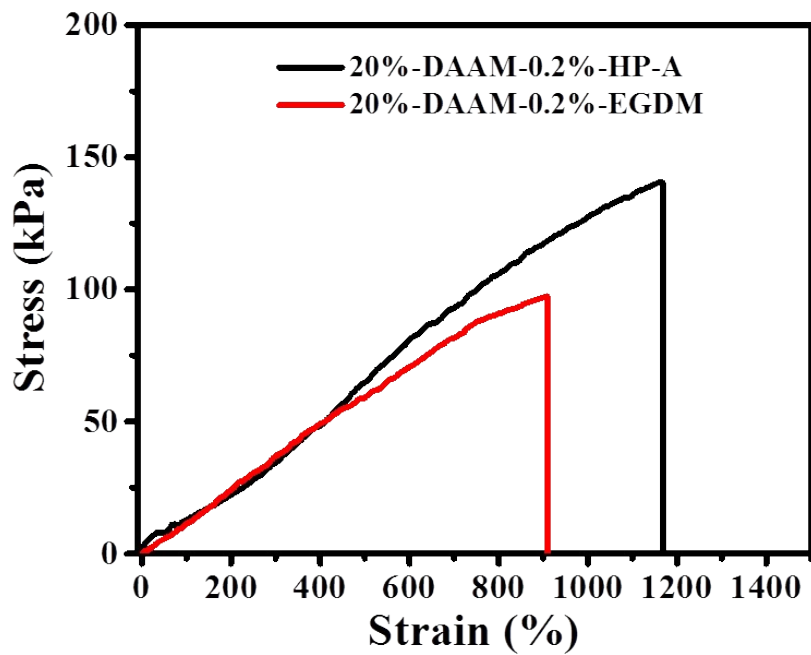


Fig. S5 Typical monotonic tensile stress-strain curves of the ionogel with HP-A and EGDM.

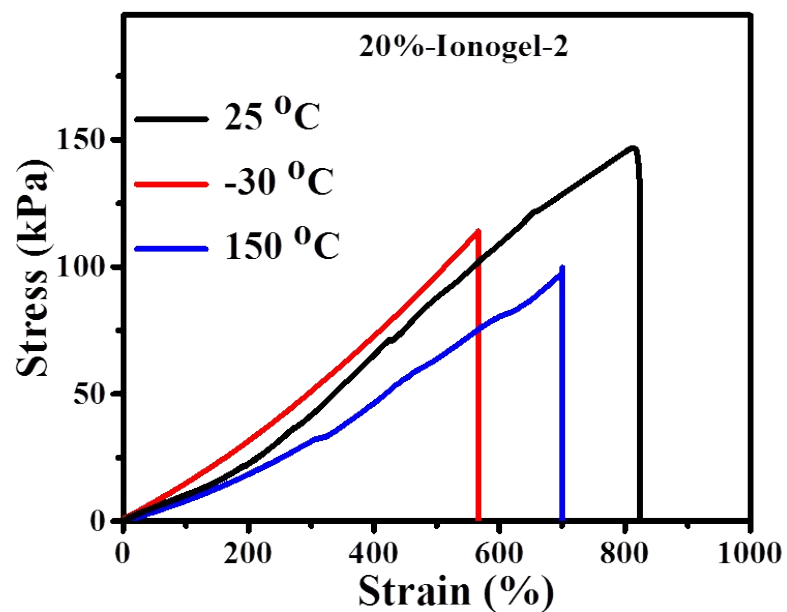


Fig. S6 Monotonic Tensile stress-strain curves of 20%-Ionogel-2 at -30 °C, 25 °C, and 150 °C.

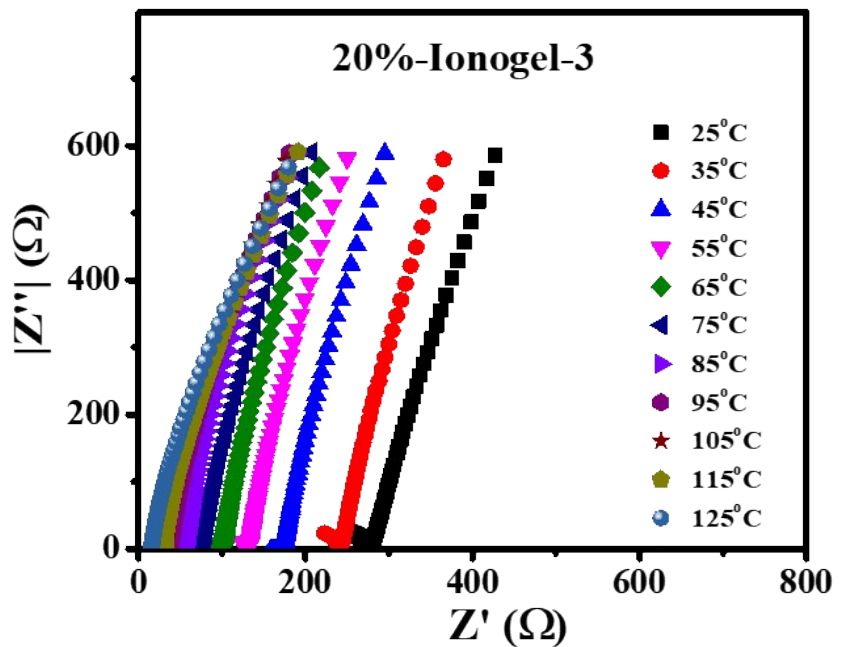


Fig. S7 The temperature dependence of impedance for 20%-Ionogel-3.

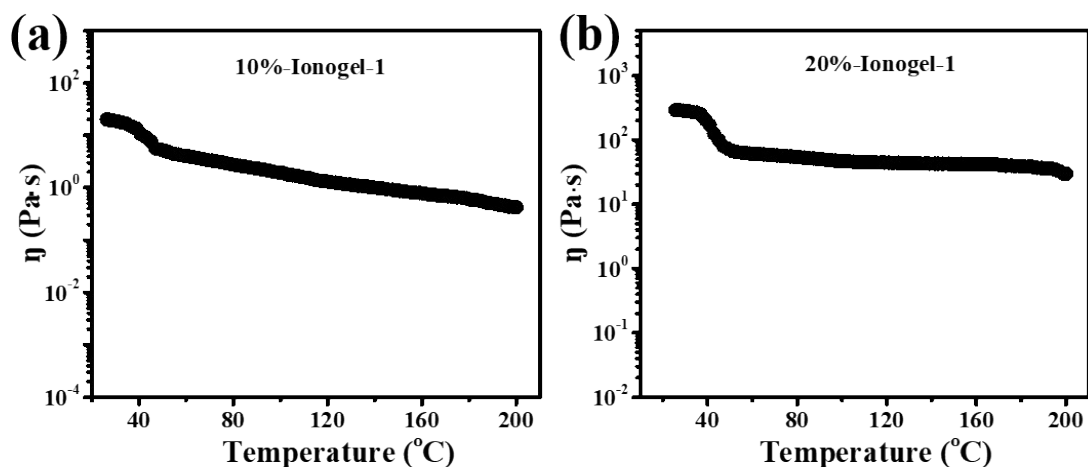


Fig. S8 The temperature dependence of viscosity for (a) 10%-Ionogel-1 and (b) 20%-Ionogel-1.

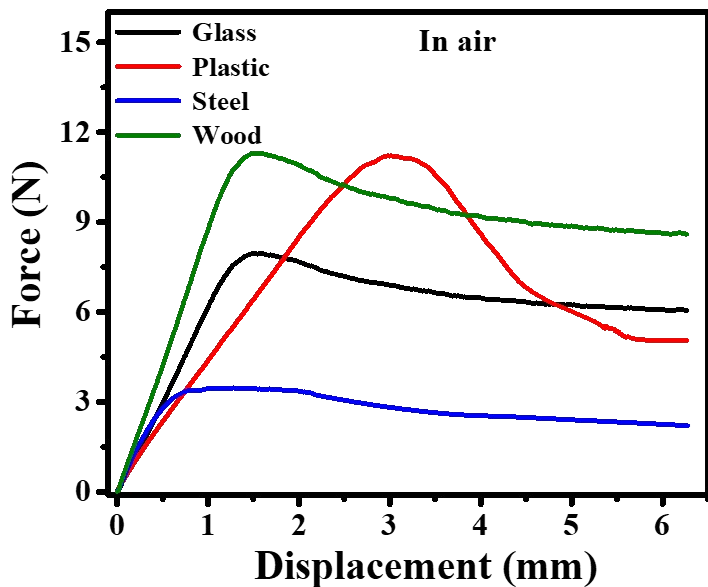


Fig. S9 Typical lap shear curves of ionogel with various substrates in air.

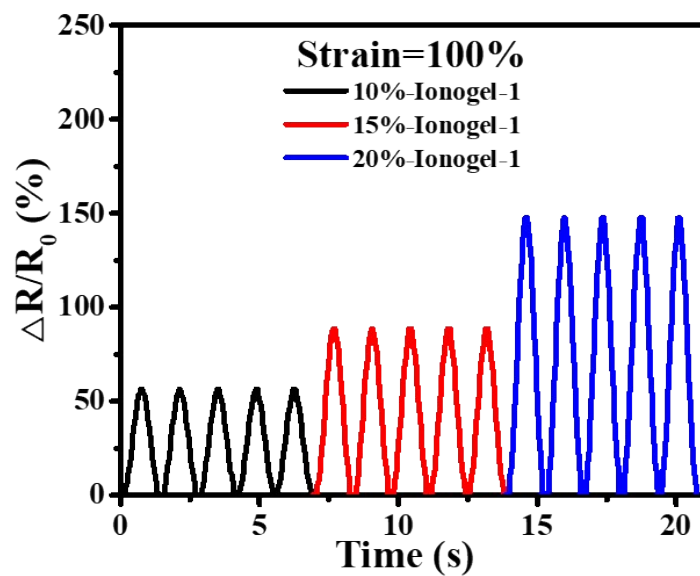


Fig. S10 The relative resistance ($\Delta R/R_0$) of the sensors with different content of DAAM (strain=100%).

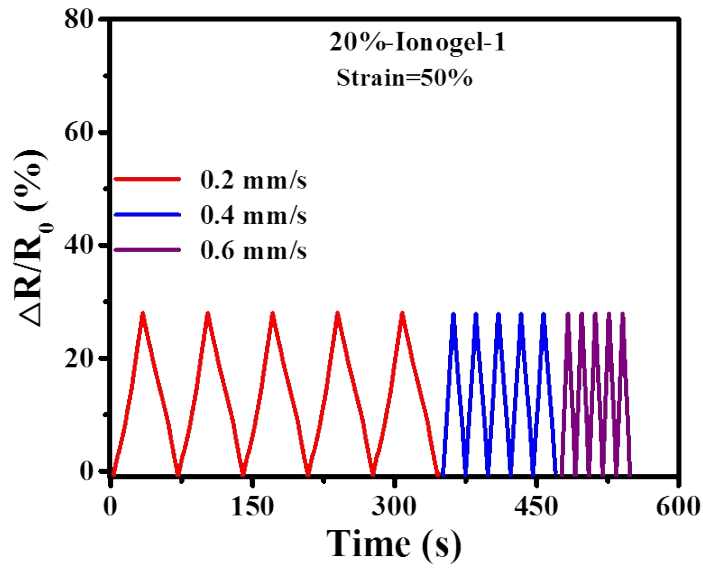


Fig. S11 The relative resistance variations ($\Delta R/R_0$) of the sensor at various loading rates.